

## RESEARCH ARTICLE

## Synthesis, characterization, and cytotoxicity of titanium dioxide nanoparticles and *in vitro* study of its impact on lead concentrations in bovine blood and milk

Murtaza Hashem, Hassan Al-Karagoly\*

Department of Internal and Preventive Medicine, College of Veterinary Medicine, University of Al-Qadisiyah, Al-Diwaniyah 58001, Iraq.

Received: May 10, 2021; accepted: May 25, 2021.

The widespread use of titanium dioxide (TiO<sub>2</sub>) nanoparticles (NPs) in various products and industrial applications has intensified the need to consider their role in treating heavy metal toxicity. Likewise, the harmful impacts of lead on the environment, animals, and humans have compelled researchers to develop more efficient, cost-effective, and environmentally friendly solutions to the issue of lead poisoning. The current study aimed to look at the cytotoxicity of titanium dioxide nanoparticles (TiO<sub>2</sub> NPs) and their ability to neutralize lead toxicity in cultured L929 cell lines, blood, and raw milk. For this purpose, fifty blood samples and twenty-five raw milk samples were collected from cattle. TiO<sub>2</sub> Nps were synthesized by the sol-gel method and characterized by the methods of Field emission scanning electron microscope (FESEM), X-ray diffraction (XRD), Energy dispersive X-ray (EDX), Fourier-transform infrared spectroscopy (FTIR), Dynamic light scattering (DLS), and Zeta potential. Pure 47 nm spherical to oval particles were synthesized. After 24, 48, and 72 hours, the TiO<sub>2</sub> NPs had no cytotoxic effect at different concentrations on L929 cell lines, whereas Pb (NO<sub>3</sub>)<sub>2</sub> was toxic to L929 cell lines resulting in a 43% reduction in their viability. TiO<sub>2</sub> NPs neutralized the toxicity of Pb (NO<sub>3</sub>)<sub>2</sub> on the L929 cell line. The mean serum lead (Pb) concentrations were remarkably reduced in both male and female cattle from 7.03±1.84 and 4.34±1.21 µg/dL to 0.47±0.38 and 0.33±0.28 µg/dL, respectively, after TiO<sub>2</sub> NPs were added. Furthermore, after TiO<sub>2</sub> NPs were added, the mean lead concentrations in raw milk decreased dramatically from 1.52±0.22 to 0.23±0.19 µg/dL. The TiO<sub>2</sub> NPs are non-cytotoxic substance and can efficiently modulate the bioavailability of lead in blood and raw milk, making it a promising method to reduce the problem of lead poisoning in animals.

**Keywords:** titanium dioxide nanoparticles (TiO<sub>2</sub> NPs); lead toxicity; L929 cell lines; blood; raw milk.

\*Corresponding author: Hassan Al-Karagoly, Department of Internal and Preventive Medicine, College of Veterinary Medicine, University of Al-Qadisiyah, Al-Diwaniyah 58001, Iraq. Phone: +964 780 440 6478. Email: [hassan.aliwee@qu.edu.iq](mailto:hassan.aliwee@qu.edu.iq).

### Introduction

Since antiquity, lead (Pb) toxicity has been recognized. The lead poisoning is one of the most common environmental diseases affecting numerous animal species and human beings worldwide [1]. The most frequent causes of lead poisoning in livestock are old lead-acid car batteries. Other lead sources for domestic animal

poisoning include lead-based paints, used engine oils, car grease and oil filters, shotgun pellets, solder, lead linoleum windows, smelter discharges, and automotive exhaust [2]. Among domestic animals, cattle have been the most frequently affected due to their high vulnerability, natural curiosity, licking, and indiscriminate eating habits [3]. Lead is initially transmitted through the blood to soft tissues,

kidneys, and liver after absorbed from the gastrointestinal tract. Lead is redistributed from soft tissues to bone in the second step. Some of the ingested lead is excreted in bile, urine, and milk [4]. Due to food safety problems and possible health threats, lead in milk draws public interest as it is widely spread in the environment. The accumulation of these heavy metals in food poses a significant risk of long-term toxicological effects [5]. The normal value for lead in milk was 100  $\mu\text{g}/\text{dL}$  according to Codex 2000. However, in 2007, the limit was lowered to 2  $\mu\text{g}/\text{dL}$  [6, 7]. There is no such amount of lead that seems to be necessary or advantageous to the body, and there has been no "safe" level of lead exposure found. Lead toxicity is an especially insidious risk. However, due to its low elimination rate, harmful lead levels can build up in tissues after sustained exposure to low lead concentrations [8].

Researchers are challenging to design scientific methods that reduce the risks of lead poisoning and find a solution to this problem due to the significant dangers posed by high levels of lead in animals' bodies and the remedial issues that result. The application of nanotechnology and nanoparticles use one of the most promising solutions [9]. Nanoparticles exhibit more physicochemical characteristics than mass materials because of their much larger surface-to-volume ratio, significantly greater reactivity, controlled particle size, site of release and site-specificity, more excellent bioactivity, low bulkiness, and speedy arrival of medications [10]. Titanium dioxide nanoparticles ( $\text{TiO}_2$  NPs) are studied as a possible photosensitizer [11]. The photocatalytic behavior of  $\text{TiO}_2$  NPs has been extensively studied to enhance the properties of medical applications. As previously mentioned, photocatalysis made use of photons and a catalyst [12], which were used to treat skin conditions and demonstrated actions against bacteria in many *in vitro* and *in vivo* toxicology tests, among them,  $\text{TiO}_2$  NPs were employed as "control" due to their low solubility and low toxicity [12]. In developing heavy metal removal technologies, nanomaterials have played a critical role [13]. Therefore, the objectives of this

study were to evaluate the cytotoxicity of  $\text{TiO}_2$  NPs and test their effects on the removal of lead toxicity from bovine blood and raw milk.

## Material and methods

### Sample collection

The animal samples were collected under the permission of the ethical committee of the College of Veterinary Medicine, University of Al-Qadisiyah (Ref. No. 82/2020), Al-Diwaniyah, Iraq.

A total of 50 cattle blood samples were collected. The blood samples were split equally between males and females. The age of animals ranged from 6 months to 6 years for both genders. Samples were obtained from the northwest, southeast, and center of Al-Diwaniyah province, Iraq. Blood samples were taken from the tail vein using a vacutainer tube after washing the region with 70% alcohol. The blood samples were then transferred to the laboratory using a cold chain. The blood samples were centrifugated at 4,000 rpm for 10 minutes to separate serum. At this stage, the clear obtained serum is ready for evaluation of lead (Pb) concentrations ( $\mu\text{g}/\text{dL}$ ) using Shimadzu AA-7000 atomic absorption spectrometry (Shimadzu, Kyoto, Japan).

Twenty-five milk samples were collected from healthy dairy cows in Al-Diwaniyah province, Iraq. The milk samples were collected using 50 mL falcon tubes. Samples were rinsed in a 10% nitric acid solution and then distilled water before each experiment. All milk samples were processed at  $-20^\circ\text{C}$  in clean containers and outside light exposure.

### Synthesis of $\text{TiO}_2$ NPs powder

$\text{TiO}_2$  NPs have been manufactured according to the previously described Sol-Gel technique [14]. At room temperature, 80 mL of isopropanol and 20 mL of titanium isopropoxide (Sigma-Aldrich, St. Louis, MO, USA) were mixed in a beaker for 5 minutes to create a homogenized solution using a magnetic stirrer. A 20 mL of deionized water was mixed with 20 mL of isopropanol in a second

beaker for 5 minutes with a magnetic stirrer. The contents of the second beaker were then added to the first beaker. At this stage, the solution obtained was milky in color. Hydrochloric acid was added dropwise to the suspension above to achieve the appropriate pH of 2-4. During this stage, the resulting suspension was mixed on a 500 rpm magnetic stirrer for 2 hours, and then, sonicated for 32 minutes to complete the homogenization reaction. The sol-gel was formed about 48 h. The solution is converted to gel at this point, and its viscosity increased. The resulting gel was then heated to 110°C for 2 hours to make it dry. Finally, the dry gel is heated in a muffle furnace at 500°C for 5 hours to produce a fine powder.

### Characterization of TiO<sub>2</sub> NPs

#### (1) X-Ray powder diffraction (XRD) assay

Applications of Cu-K $\alpha$ -wavelength ( $\lambda$ = 1.5405 Å) were produced by using a Phillips diffractometer (Malvern Panalytical, Worcestershire, UK) in powder samples of TiO<sub>2</sub> NPs. The voltage used was 40 kV, and the current intensity was 25 mA. XRD is essential for determining the crystal structure, size, and crystallinity of a sample using the Scherrer equation:

$$D = K\lambda / \beta \cos\theta$$

K is a dimensionless constant,  $\lambda$  is the X-ray radiation distance,  $\beta$  is the diffraction peak's full width at half limit (FWHM), and  $\theta$  is the diffraction angle.

A crystallite's size is determined by expanding a certain peak in a diffraction pattern associated with a particular planar reflection inside the crystal unit. The FWHM of a single height is inversely proportional, the lower the peak, the larger the crystallite volume.

#### (2) Field emission scanning electron microscope (FESEM)

The morphological features and size of TiO<sub>2</sub> NPs were studied by using MIRA3 TESCAN-XMU FESEM (HORIBA Scientific, Kyoto, Japan) under a 20 kV electron acceleration.

#### (3) Dynamic light scattering (DLS) measurement

The fabricated TiO<sub>2</sub> NPs were measured by DLS using Horiba SZ-100 nanoparticle analyzer (Horiba, Kyoto, Japan). An appropriate powder concentration of 0.01 g/100 mL was distributed in Dimethyl sulfoxide (DMSO). The medium had been used to estimate the cytotoxicity effect on DMSO distribution particles.

#### (4) Zeta analysis

Zeta potential measurement was performed by using Horiba SZ-100 nanoparticle analyzer to investigate the particles' surface charge of prepared TiO<sub>2</sub> NPs. The particles' electrostatic potential was determined in DMSO at room temperature using ultrasonic dispersion of 0.01 g/100 mL.

#### (5) Fourier-transform infrared spectroscopy (FTIR) analysis

Shimadzu FTIR system (Shimadzu, Kyoto, Japan) was used to evaluate the prepared samples' functional groups over a wavelength range of 400-4,000 /cm.

### Cell Culture and 3-(4,5-dimethylthiazol-2-yl)-2,5-diphenyltetrazolium bromide (MTT) assay

#### (1) Cytotoxicity of TiO<sub>2</sub> NPs

Mouse fibroblast (L929) cells (Central Laboratory, Isfahan Technology University, Isfahan, Iran) were cultivated in Dulbecco's modified eagle medium (DMEM) (Sigma-Aldrich, St. Louis, MO, USA) with 100 U/mL penicillin, 100 g/mL streptomycin, and 10% fetal bovine serum (FBS) at 37°C and 5% CO<sub>2</sub> humidification. In the MTT experiments, the cells were seeded in the 96-well plates with density of 3.0×10<sup>5</sup> cell/well. TiO<sub>2</sub> NPs have been diluted to a reasonable concentration of 5, 10, 25, 50, and 100 µg/mL for a freshly distributed in a cell culture setting for 24, 48, and 72 h. Each well was washed twice with phosphate-buffered saline (PBS) before adding fresh 100 mL of culture medium and 0.5 mg/mL of MTT reagent. After that, the labeled cells were incubated at 37°C under 5% CO<sub>2</sub> for 4 h. After replacing the medium with 100 µg/mL fresh DMSO, the OD was measured using an ELISA plate reader (Bio-Rad, Hercules, CA, USA) at 570

nm after 10 minutes of trembling. The data were recorded as the mean  $\pm$  SD where the cell culture without TiO<sub>2</sub> NPs acted as a control. All experiments had been triplicated.

### **(2) Cytotoxicity of lead nitrate (Pb(NO<sub>3</sub>)<sub>2</sub>)**

MTT experiments were applied to detect the proliferation of L929 cells cultivated in media with various concentrations of Pb(NO<sub>3</sub>)<sub>2</sub> (10, 20, 40, 80, 160  $\mu$ g/mL). Cells were cultured in 96-well plate at a density of  $3.0 \times 10^5$  cells per well. 20  $\mu$ L of 5 mg/mL MTT in 0.01 M PBS solution were added to each well. The plate was incubated at 37°C under 5% CO<sub>2</sub> for 4 hours. The purple products were then carefully removed and transferred into 0.2 mL of DMSO. OD<sub>570</sub> was measured by using the ELISA plate reader (Bio-Rad, Hercules, CA, USA). All the experiments were carried out three times. The mean  $\pm$  SD was used to describe the data with the cell culture without Pb(NO<sub>3</sub>)<sub>2</sub> as the control.

### **(3) The effect of TiO<sub>2</sub> NPs on the cytotoxicity of Pb(NO<sub>3</sub>)<sub>2</sub> on L929 cell line**

The MTT assay was used to test TiO<sub>2</sub> NPs to neutralize the Pb(NO<sub>3</sub>)<sub>2</sub> toxic effect on L929 cells. L929 cells were cultured with the media containing Pb(NO<sub>3</sub>)<sub>2</sub> and TiO<sub>2</sub> NPs (1:1) at various concentrations of 10, 20, 40, 80, 160  $\mu$ g/mL for 24, 48, and 72 h. After treatment, a total volume of 20  $\mu$ L media (5 mg/mL MTT in 0.01 M PBS) was added to each well and continued incubation under 5% CO<sub>2</sub> at 37°C for 4 hours. The medium was then carefully aspirated, and 0.2 mL of DMSO was applied to dissolve the purple materials. OD<sub>570</sub> was measured using the same plate reader after shaking the plate for 10 minutes. A triplicate assay was achieved for all samples. Data was shown as mean  $\pm$  SD. Cells cultivated in media with no Pb(NO<sub>3</sub>)<sub>2</sub> and TiO<sub>2</sub> added were set as the control.

### **(4) Determination of Pb concentration in blood and raw milk samples**

The furnace atomic absorption spectrometry (FAAS) was used to determine the lead concentrations in blood and milk samples. 2 mL of serum was diluted with 15 mL of distilled

water, then 8 mL concentrated nitric acid was added. During gentle mechanical shaking for 5 minutes, 1 mL of 30% H<sub>2</sub>O<sub>2</sub> was added to the sample. The sample was diluted with distilled water to 25 mL before ultrasonic analysis at 60°C for 30 minutes. All the samples were carried out in a triplicate manner. For the milk sample, a total amount of 6 mL (2 mL raw milk and 4 mL purified water) was combined with 4 mL of 65% nitric acid and incubated for 24 hours at 85°C. Subsequently, 4 mL of 30% hydrogen peroxide was added and the sample was set at 120°C for 1 h in the semi-closed glass digester. Finally, the reaction was diluted by adding 10 mL of 1% nitric acid, and the volume of lead was determined by furnace atomic absorption spectrophotometry. A triplicated pattern was applied to all samples [16].

### **(5) The effects of TiO<sub>2</sub> NPs to Pb in serum and milk samples**

A 0.2 mL of formulated TiO<sub>2</sub> NPs (47 nM, 99% purity) was applied to 2 mL of serum and 2 mL of milk samples, respectively to measure the elimination of Pb by TiO<sub>2</sub> NPs. The sample was then put under UV light (315-400 nm, 40W) for 2 hours to complete the oxidation reaction. Finally, the remaining amount of Pb was calculated by using furnace atomic absorption spectrometry. Both serum and milk samples were performed in triplication.

### **Statistical analysis**

The data were shown in terms of mean  $\pm$  SD, and the variations were considered significant when  $P < 0.05$ . The data was analyzed using Microsoft Excel and SPSS statistic tools (V.22) (IBM, Chicago, IL, USA).

## **Results**

### **Characterization of TiO<sub>2</sub> NPs**

#### **(1) The field emission scanning electron microscope (FESEM)**

The synthesized TiO<sub>2</sub> NPs with an average of 47 nm of relatively ovoid shape were shown in Figure 1 by using FESEM technique.

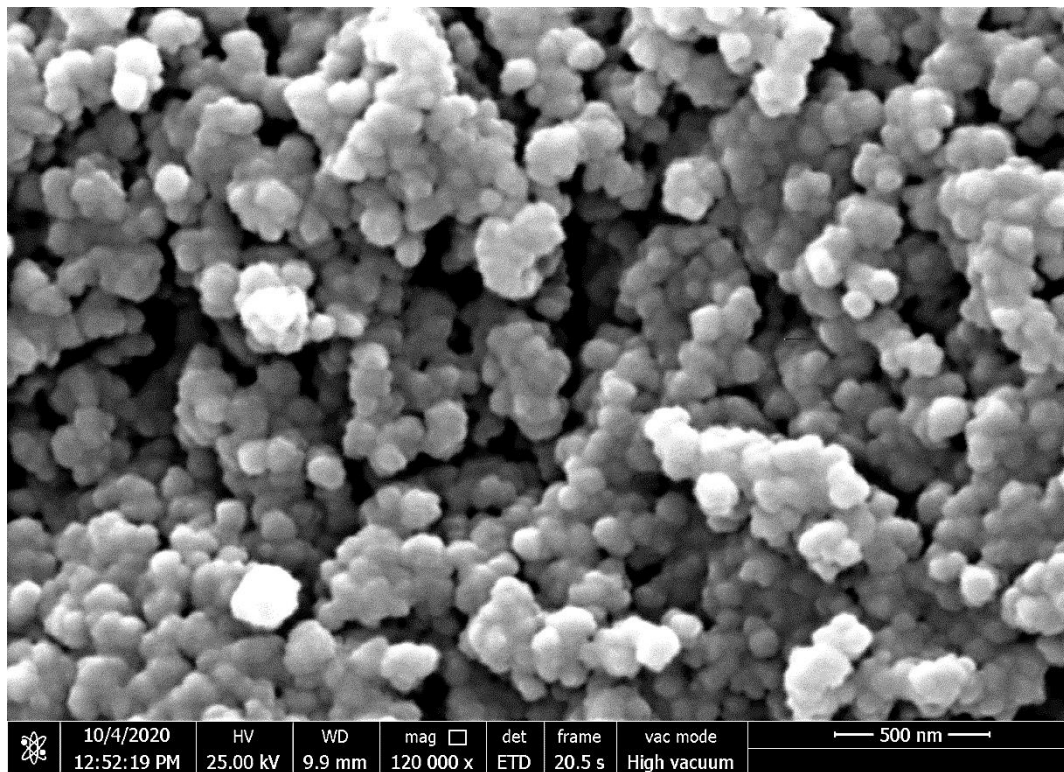


Figure 1. FESEM image showed a spherical to the ovoid shape of synthesized TiO<sub>2</sub> NPs.

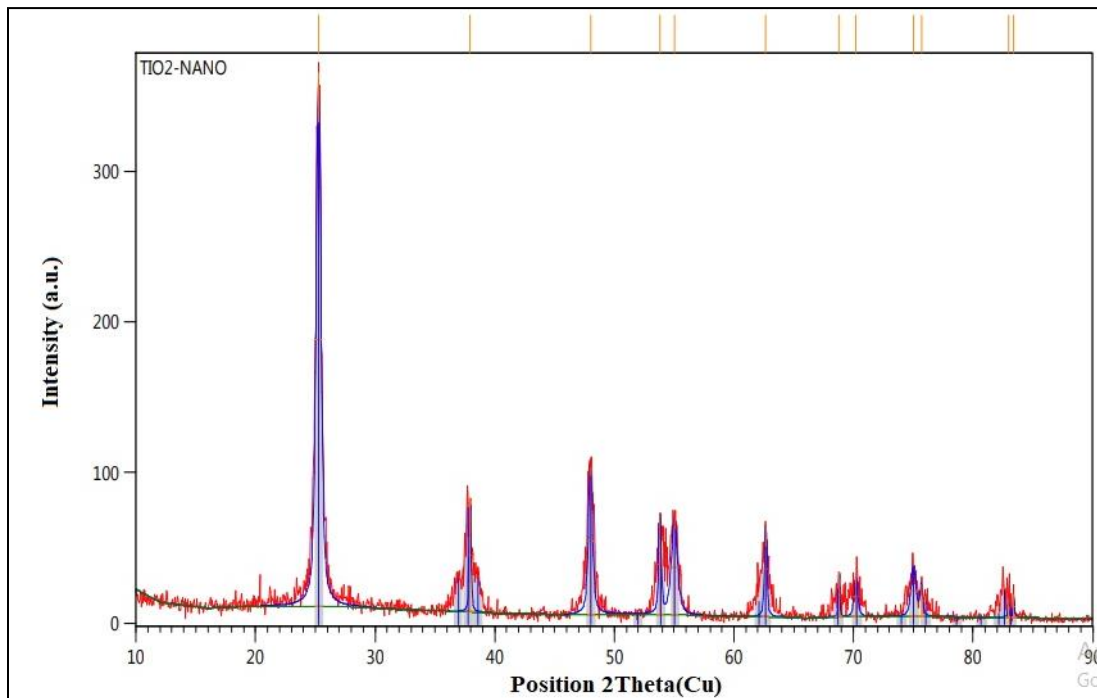


Figure 2. XRD pattern of prepared TiO<sub>2</sub> NPs by sol-gel method.

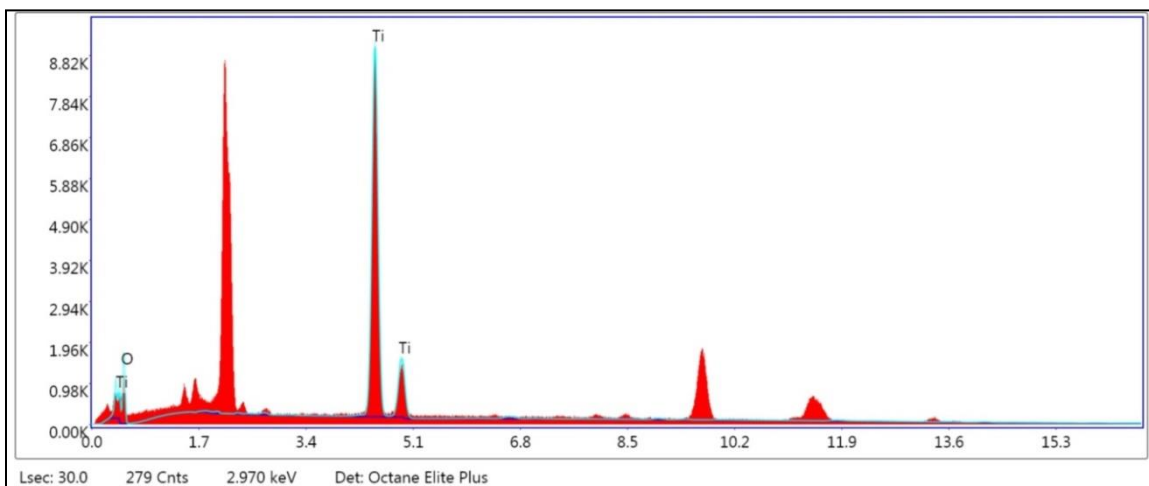


Figure 3. EDX spectrum of TiO<sub>2</sub> nano-composition.

## (2) X-ray powder diffraction (XRD)

In XRD patterns, the calcined temperature (400°C) of TiO<sub>2</sub> NPs was shown. The TiO<sub>2</sub> NPs were anatases when the heating temperature was increased to 400°C. The diffraction peaks at 2.5, 37.9, 48.2, 53.8, 62.6, 70.14, 75.66, and 83.10°C matched the crystal plane patterns of (101), (004), (200), (105), (211), (204), (220), (215), and (312), which were characteristics of TiO<sub>2</sub> NPs' anatase process (Figure 2).

## (3) Analysis of energy dispersive X-Ray (EDX)

The EDX spectra confirmed the pure TiO<sub>2</sub> nanocomposite process, describing the elemental composition of nanoparticles' samples in Figure 3.

## (4) Dynamic light scattering and zeta analysis (DLS)

Dynamic light scattering (DLS) was performed on samples dispersed in DMSO to evaluate their average hydrodynamic radius and to confirm the above FESEM particle sizing measurements. Several samples were readily accumulated in the DMSO as demonstrated by a slightly greater particle size than FESEM particle counting and a large particle size variance. All substances were found to be ovoid nanoparticles, with a mean FESEM particle size of 0.40–0.49 anisotropy. In general, DLS data agreed with FESEM particle sizes.

DLS determined the particle size and Zeta potential for TiO<sub>2</sub> NPs. The Zeta potential below -25 mV and above +25 mV suggested a stable surface of nanoparticles without a propensity to accumulate. Lower Zeta potential values indicated nanoparticle aggregation due to Van der Waals forces. In Figure 4, Zeta potential values of -49.1 mV for TiO<sub>2</sub> NPs was observed, corresponding to stable DMSO dispersions. The Zeta potential with a negative value of -49.1 mV and electrophoretic movement (mean) of -0.000380 cm<sup>2</sup>/Vs was a good predictor for equilibrium without particle settlement of TiO<sub>2</sub> NPs suspension in DMSO. The prepared suspension report also showed that the general zeta potential conditions for increased stability were negative. It was investigated if prepared TiO<sub>2</sub> NPs in DMSO had a hydrodynamic scale. DLS demonstrated a relatively thin body with a hydrodynamic diameter of 180 nm (Figure 5).

## (5) Fourier-transform infrared spectroscopy (FTIR) analysis

The functional groups of TiO<sub>2</sub> NPs were calculated by FTIR analysis. Related absorption peaks observed in the synthesis of TiO<sub>2</sub> visible light active and magnetically recyclable nanocomposite have been documented by Helin Niu, *et al.* [15]. The TiO<sub>2</sub> nanocomposite FTIR transmission spectrum was shown in Figure 6. The wideband based at 500-600/cm was

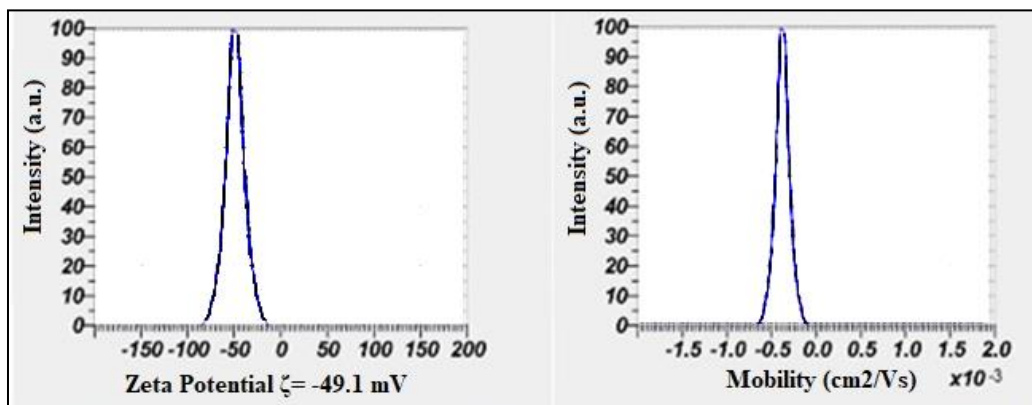


Figure 4. Zeta potential analysis ( $\zeta = -49.1$  mV) of prepared TiO<sub>2</sub> NPs.

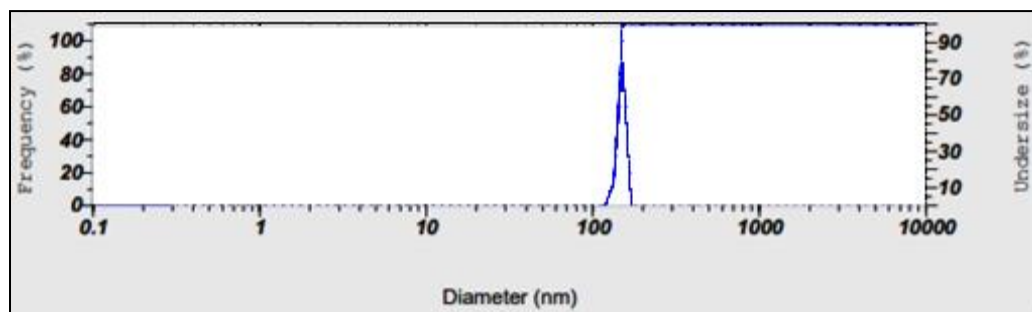


Figure 5. DLS image of the particle volume distribution size of TiO<sub>2</sub> NPs.

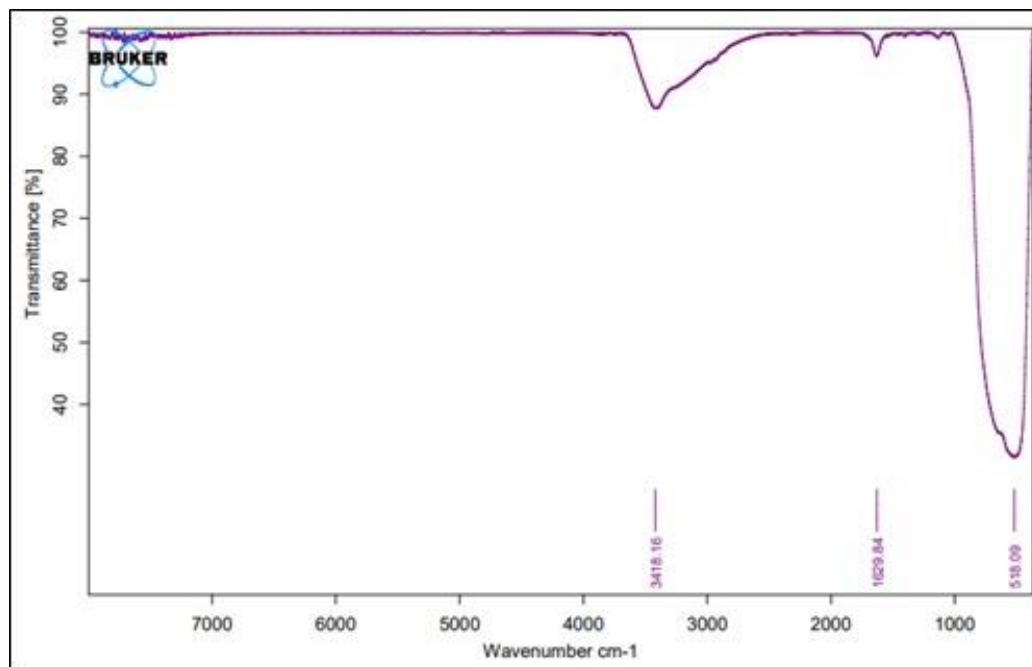


Figure 6. FTIR spectrum of anatase TiO<sub>2</sub> NPs confirmed relative functional groups.

allocated to bending vibration (Ti-O-Ti) bonds in the TiO<sub>2</sub> lattice. For the hydroxyl group, intermolecular interaction of the water molecule with the surface of TiO<sub>2</sub>, broadband of 3,600-3,400/cm was chosen. The peak at 1,650/cm corresponds to the OH group's bending vibration characteristic.

### MTT assays

#### (1) Cytotoxicity of TiO<sub>2</sub> NPs

The viabilities of L929 cells cultured in media containing various TiO<sub>2</sub> NPs concentrations for 24, 48, and 72 h were determined by using MTT assay. The cells retained their vitality for 24 hours at different concentrations, close to the control group. However, the cells' vitality decreased by 4.59% and 6.68 % over 48 and 72 hours at elevated concentrations of TiO<sub>2</sub> NPs (100 µg/mL) (Figure 7). The results showed a correlation between L929 cell viability and the concentration of TiO<sub>2</sub> NPs in a dose-dependent manner, where the cell viability slightly nonsignificant decreased at high concentrations of TiO<sub>2</sub> NPs.

#### (2) Cytotoxicity of Pb(NO<sub>3</sub>)<sub>2</sub>

In response to various Pb(NO<sub>3</sub>)<sub>2</sub> concentrations present in the culture medium, the MTT assay evaluated cell proliferation. The viability of the cultured cells was greatly affected as the Pb(NO<sub>3</sub>)<sub>2</sub> concentration in the culture medium increased from 10 to 160 µg/mL. However, substantial cytotoxicity of Pb(NO<sub>3</sub>)<sub>2</sub> was observed at 160 µg/mL concentration after 72 h of cell culture (Figure 8). Cells cultured in a medium containing 160 µg/mL Pb(NO<sub>3</sub>)<sub>2</sub> for 72 h demonstrated 43.75% cytotoxicity comparing to the control group.

#### (3) The effect of TiO<sub>2</sub> NPs on Pb(NO<sub>3</sub>)<sub>2</sub> cytotoxicity in L929 cell line

The TiO<sub>2</sub> NPs demonstrated a protective effect, which the cell viability was preserved and the toxic effect of Pb(NO<sub>3</sub>)<sub>2</sub> was prevented at less than 5.19% level, even at the high concentration of Pb(NO<sub>3</sub>)<sub>2</sub> (160 µg/mL). There was also an upward trend observed with rising concentrations (Figure 8).

#### (4) Concentrations of Pb in blood samples

The findings of the current study showed that the mean serum Pb concentration was 7.03±1.84 µg/dL (ranged from 2.25 to 9.22 µg/dL) and 4.34±1.21 (ranged from 2.28 to 6.68 µg/dL) in males and females, respectively. The statistical analysis of Pb levels showed a significant difference between males and females (P < 0.05), as the serum concentrations of lead in males were higher than that in females, while toxicity levels had not been reported. After adding TiO<sub>2</sub> NPs to the same serum samples, the concentrations of serum Pb in males and females were significantly decreased to 0.47±0.38 and 0.33±0.28 µg/dL, respectively (P < 0.05).

#### (5) Concentrations of Pb in raw milk samples

The present study results showed that the mean Pb concentration in raw milk was 1.52±0.22 µg/dL (ranged from 1.12 to 2.14 µg/dL). Lead concentrations in raw milk samples were significantly decreased to 0.23±0.19 µg/dL after processing with TiO<sub>2</sub> NPs (P < 0.05).

### Discussion

The morphology of TiO<sub>2</sub> NPs was determined by using FESEM. The TiO<sub>2</sub> NPs had an uneven morphology due to the primary particle's agglomeration, which had an average diameter of 47 nm. In this case, the fine particles ranged in size between 31 and 96 nm, and the coarse particles were in the 100 to 200 nm range. Since the fine particles easily bind together and form the coarse particle, the particle observed from FESEM morphology analysis was large. According to the TiO<sub>2</sub> Manufacturers Association, chemical bonds bind the particles together to form aggregates. These aggregates appear to clump together due to Van-der Waals's attraction, forming particles larger than 100 nm [16].

The XRD pattern of TiO<sub>2</sub> NPs calcined at 400°C was reported in the current study. After calcination, anatase peaks of TiO<sub>2</sub> powder were obtained. The XRD pattern matched the JCPDS card no. 21-1272 (anatase TiO<sub>2</sub>) and the graphs'

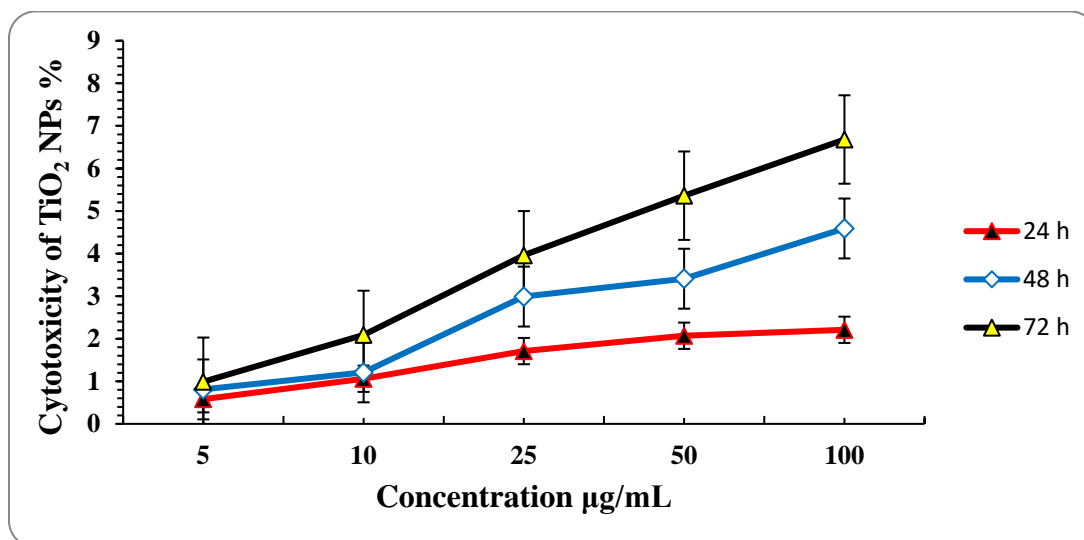


**Figure 7.** The viability of L929 cells cultured in media containing various TiO<sub>2</sub> NP concentrations and different incubation time (24, 48, and 72 h). The cells retained their vitality for 24 hours at different concentrations. However, the cells' vitality decreased by 4.59 and 6.68% over 48 and 72 hours at elevated concentrations of TiO<sub>2</sub> NPs (100 µg/mL). The data is presented as a mean ± standard deviation.

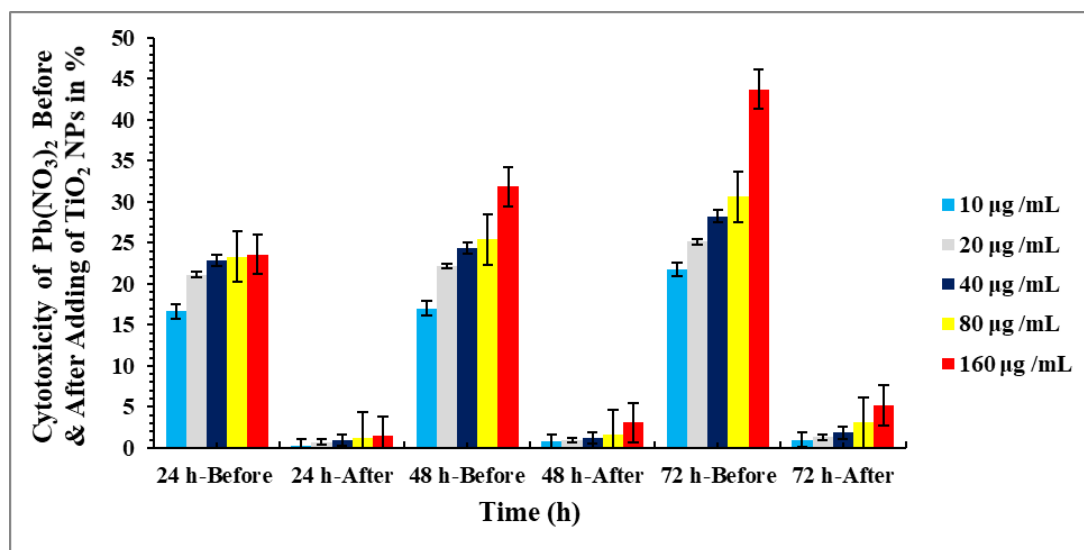


**Figure 8.** The cytotoxicity of Pb(NO<sub>3</sub>)<sub>2</sub> before and after adding TiO<sub>2</sub> NPs in the cultivation media of the L929 cell line. The MTT tests was performed in media containing various concentrations of TiO<sub>2</sub> NPs and Pb(NO<sub>3</sub>)<sub>2</sub> (10, 20, 40, 80, 160 µg/mL) and during different treatment times (24, 48, and 72 hours).

peaks were in solid harmony with previous analysis. It can be assumed that titanium at 25.2°C with 2θ, the material presents at the stoichiometric proportion (101), and the absence of spurious diffractions shows crystallographic purity [17].

The presence of characteristic titanium (TiO<sub>2</sub>) peak at 2.970 keV in the EDX results suggested that the electron-dense regions seen in the FESEM image were TiO<sub>2</sub> particle aggregates. EDX may be used to assess the aggregates' elemental composition. According to the X-ray mapping, the particles were titanium and oxygen-enriched,

meaning that the FESEM picture particles were TiO<sub>2</sub> particles [18].

Dynamic light scattering (DLS) and Zeta Potential Analysis were performed on samples dispersed in DMSO to evaluate their average hydrodynamic radius and confirm the FESEM particle sizing measurements. Several samples were readily accumulated in the DMSO, as demonstrated by a slightly greater particle size than FESEM particle counting and a large particle size variance. All substances were found to be ovoid nanoparticles with an average FESEM particle size of 0.40–0.49 anisotropy. In general, DLS data agreed with FESEM particle sizes.

The prepared suspension showed that the general zeta potential conditions for increased stability were negative [19]. It was investigated that the prepared TiO<sub>2</sub> NPs in DMSO had a hydrodynamic scale. DLS demonstrated a relatively thin body with a hydrodynamic diameter of 180 nm. Zhang, *et al.* confirmed the substance's zeta potential for understanding the nature of cell interactions, cell diagnosis, and normal and cancer-cell effect therapeutics [20].

The FTIR spectra of TiO<sub>2</sub> NPs were shown in Figure 6. Three bands were visible in the FTIR spectrum of TiO<sub>2</sub> NPs. FTIR analysis was used to determine the functional groups of TiO<sub>2</sub> NPs. Helin Niu, *et al.* [15] reported related absorption peaks observed in the synthesis of TiO<sub>2</sub> visible light active and magnetically recyclable nanocomposite. The bending vibration (Ti-O-Ti) bonds allocated to the TiO<sub>2</sub> lattice showed wideband based at 500-600/cm. Bending vibration (Ti-O-Ti) connections within the TiO<sub>2</sub> grid were assigned to the broadband at a range of 500-600/cm. The water molecule's intermolecular interaction with the surface of TiO<sub>2</sub> was chosen for the hydroxyl group with a broadband of 3,600-3,400/cm. At 1,650/cm, a characteristic peak formed corresponding to the OH group's bending vibration [21].

An earlier study suggested that the degree of toxicity of TiO<sub>2</sub> NPs depended on the cells

involved and concentrations of the particles [22], made inter-study comparison of TiO<sub>2</sub> NP toxicity difficult. Although some other studies reported zero or only a slight depletion in cell viability, it is consistent with our findings [23]. According to our results, treatment of L929 mouse fibroblast cell lines with TiO<sub>2</sub> NPs at concentrations ranging from 5 to 100 µg/mL showed no significant cytotoxicity [22]. The researchers found TiO<sub>2</sub> NPs increased cells' viability in a dose-dependent manner, much like the recent study that TiO<sub>2</sub> NPs promoted cell viability and proliferation in NIH 3T3 cells [24]. Cell viability assays using MTT in exposed cells showed concentration and cell type-dependent cytotoxicity and proliferation. According to Huang, *et al.*, treatment of HCT116 cell with TiO<sub>2</sub> NPs resulted in significant survival and growth, which was consistent with a recent study that found TiO<sub>2</sub> NPs promoted cell viability and proliferation in NIH 3T3 cells in a time- and dose-dependent manner [24]. Cell viability of cultured human vascular endothelial cells was not substantially diminished as the concentration of TiO<sub>2</sub> NPs increased, where no significant cytotoxicity was observed following the L929 mouse fibroblast cell line [22].

Data from the current study indicated that Pb(NO<sub>3</sub>)<sub>2</sub> was highly cytotoxic to L929 cells. These findings supported those of a previous study that found that higher levels of lead reduced the viability of HepG2 cells significantly [25]. Even though our results agreed with previous investigations that reported a reduction in cancer cells' viability following exposure to lead [26], a recent study found that Pb affected each organ system in the body that was susceptible to the effects of lead toxicity including hematopoietic, cardiovascular, kidney, and skeletal systems [27]. The results of another study found an intense positive concentration-dependent relationship between elevated lead nitrate concentrations and the percentage of dead HL-60 cells treated 24 hours with three different Pb(NO<sub>3</sub>)<sub>2</sub> concentrations [28]. The current results corroborated previous studies that observed a substantial decrease in cancer cell viability after exposure to lead [29]. Comparing to the

observations, the proportion of necrotic cell death increased as lead nitrate concentrations increased, suggesting a gradual decrease in leukemic cell viability. In contrast to the control group, lead-treated cells displayed critical morphological changes. Cell necrosis and morphologically established cell death due to lead toxicity can be identified by characteristic cytological features including increased cell volume, swelling, and the rupture of plasma membrane [30].

Our findings showed that the mean Pb concentration was  $7.03 \pm 1.84 \mu\text{g/dL}$  (ranged from 2.25 to  $9.22 \mu\text{g/dL}$ ) and  $4.34 \pm 1.21$  (ranged from 2.28 to  $6.68 \mu\text{g/dL}$ ) in males and females, respectively. The lead levels' statistical analysis showed significant difference ( $P < 0.05$ ) between males and females as the lead concentrations in males were higher than it in females. Moreover, the results showed that the mean lead concentration in raw milk was  $1.52 \pm 0.22 \mu\text{g/dL}$  (ranged from 1.12 to  $2.14 \mu\text{g/dL}$ ). The current study results revealed that Pb concentrations in serum were high but less than the toxic levels. Many studies reported that Pb's toxic levels ranged between 10-30  $\mu\text{g/dL}$  [31]. Despite this, researchers are almost unanimous in believing that even low lead levels are poisonous and can cause serious health problems [32]. In the same context, our findings suggested that lead concentrations in raw milk were toxic and were consistent with those previously defined by several researchers and European Commission Regulations (2006), which indicated that the toxic concentration of Pb in raw milk is 0.02  $\mu\text{g/mL}$  [33].

The current study established a substantial difference in lead levels between males and females as the study discovered that males had significantly higher lead levels in their blood than it in females. Our results were consistent with several other studies that had been reported gender differences in toxic metal exposure, and there is growing evidence that harmful metal health effects are often expressed differently in males and females due to differences in kinetics,

mode of action, or sensitivity [34]. In general, lead blood level in male is higher than it in female, fundamentally due to higher exposure and more elevated blood hematocrit, as blood lead is bound to erythrocytes. Furthermore, antioxidant defenses with catalase activity in female are gender-related [34]. Moreover, it has been confirmed that female rats' mitochondria have higher antioxidant enzyme expression and lower reactive oxygen production than that of male mitochondria [35]. Estrogen with antioxidant effects performs additional defense against oxidative stress by acting as a scavenger or synthesizing protective molecules by activating estrogen receptors.

The current study results showed a substantial difference between Pb concentration in both males and females before and after adding  $\text{TiO}_2$  NPs, where the concentration of Pb in serum decreased to  $0.47 \pm 0.38$  and  $0.33 \pm 0.28 \mu\text{g/dL}$ , respectively. Furthermore, the concentration of Pb in raw milk was dramatically reduced after adding  $\text{TiO}_2$  NPs to  $0.23 \pm 0.19 \mu\text{g/dL}$ .  $\text{TiO}_2$  NPs successfully decreased bioaccumulation and lead concentrations in blood and raw milk in the present analysis. Current evidence indicated that  $\text{TiO}_2$  NPs could absorb metal ions in solution, including Pb, As, Cu, and Cd [36].  $\text{TiO}_2$  NPs exhibit superior optical and electrical properties. Thus, research on the application of  $\text{TiO}_2$  NP in heavy metal exposure prevention and tumor treatment is also encouraged [37]. Due to the unique properties of the  $\text{TiO}_2$  NPs such as a high surface area-to-volume ratio, good surface reactivity, excellent affinity, versatility, low cost, and non-toxicity, and its significant advantages in absorbing and concentrating chemical toxins,  $\text{TiO}_2$  NPs may ultimately benefit environment, animal, and human health. Photocatalyzed oxidation methods have been developed in which heavy metals such as titanium dioxide are oxidized with photocatalysts after being exposed to UV radiation [38]. In targeted leukemia K562 cells, the  $\text{TiO}_2$  NPs under UV radiation could increase drug accumulation and inhibit multidrug resistance. According to this finding, combining  $\text{TiO}_2$  NPs and UVA irradiation could be valuable in

tumor therapy [39]. The photocatalytic activity, coating, and doping of TiO<sub>2</sub> NPs have been extensively studied to improve potential medical applications. Photocatalysis utilizes photons and a catalyst. A semi-conductor like TiO<sub>2</sub> is used as a photocatalyst, which induces a surface oxidation-reduction (redox) reaction when UV-visible light suits its gap [41]. Oxygen on the surface of a semiconducting photocatalyst is the principal agent for the photocatalytic debasement of heavy metal pollutants. The energy consumed by the semiconducting metal oxide results in oxygen production, which aids in reducing organic and metal contaminants to less harmful products or intermediates [40]

### Conclusion

Despite the lack of toxicity levels, lead concentrations in animals' serum were high, especially in males, which showed a statistically significant difference from females. At the same time, the concentration in raw milk reached a toxic level. Aspherical, 47 nm size TiO<sub>2</sub> NPs were found to be non-cytotoxic when tested by MTT assay and effectively neutralized the cytotoxic effects of Pb(NO<sub>3</sub>)<sub>2</sub> on L929 cell lines. Furthermore, TiO<sub>2</sub> NPs potentially reduced high levels of lead in blood and raw milk to deficient levels, which makes it a promising way to contribute to eliminate the issue of lead poisoning in animals.

### Acknowledgments

We would like to thank the herd breeders who helped us collecting samples and the College of Veterinary Medicine, University of Al-Qadisiyah for providing the necessary laboratories to complete this study.

### References

1. Flora SJ, Flora G, Saxena G: Environmental occurrence, health effects and management of lead poisoning. *Lead*. Elsevier. 2006:158-228.
2. Aslani MR, Heidarpour M, Najar-Nezhad V, Mostafavi M, Toosizadeh-Khorasani Y. 2012. Lead poisoning in cattle associated with batteries recycling: High lead levels in milk of nonsymptomatic exposed cattle. *Iran J Vet Res*. 4:47-52.
3. Alloway BJ: Heavy metals and metalloids as micronutrients for plants and animals. *Heavy metals in soils*. Springer. 2013:195-209.
4. Flora SJ, Pachauri V. 2010. Chelation in metal intoxication. *Int J Environ Res Public Health*. 7:2745-2788.
5. Pšenková M, Toman R, Tančin V. 2020. Concentrations of toxic metals and essential elements in raw cow milk from areas with potentially undisturbed and highly disturbed environment in Slovakia. *Environ Sci Pollut Res*. 27:26763-26772.
6. Najarnezhad V, Akbarabadi M. 2013. Heavy metals in raw cow and ewe milk from north-east Iran. *Food Addit Contam B*. 6:158-162.
7. Ogabiela E, Udiba U, Adesina O, Hammuel C, Ade-Ajayi F, Yebpella GG, *et al*. 2011. Assessment of metal levels in fresh milk from cows grazed around Challawa Industrial Estate of Kano, Nigeria. *J Basic Appl Sci Res*. 1(7):533-538.
8. Ercal N, Gurer-Orhan H, Aykin-Burns N. 2001. Toxic metals and oxidative stress part I: mechanisms involved in metal-induced oxidative damage. *Curr Top Med Chem*. 1(6):529-539.
9. Kumar A, MMS C-P, Chaturvedi AK, Shabnam AA, Subrahmanyam G, Mondal R, *et al*. 2020. Lead toxicity: health hazards, influence on food chain, and sustainable remediation approaches. *Int J Environ Res Public Health*. 17(7):2179.
10. Num S and Useh N. 2013. Nanotechnology applications in veterinary diagnostics and therapeutics. *Sokoto J Vet Sci*. 11:10-14.
11. Ziental D, Czarczynska-Goslinska B, Mlynarczyk DT, Glowacka-Sobotta A, Stanisz B, Goslinski T, *et al*. 2020. Titanium dioxide nanoparticles: prospects and applications in medicine. *Nanomaterials*. 10:387.
12. Warheit DB, Webb TR, Reed KL, Frerichs S, Sayes CM. 2007. Pulmonary toxicity study in rats with three forms of ultrafine-TiO<sub>2</sub> particles: differential responses related to surface properties. *Toxicology*. 230:90-104.
13. Kijima T: Inorganic and metallic nanotubular materials: Recent technologies and applications. Springer Science & Business Media, 2010.
14. Priyanka KP, Sukirtha TH, Balakrishna KM, Varghese T. 2016. Microbicidal activity of TiO<sub>2</sub> nanoparticles synthesised by sol-gel method. *IET nanobiotechnol*. 10(2):81-86.
15. Niu H, Wang Q, Liang H, Chen M, Mao C, Song J, *et al*. 2014. Visible-light active and magnetically recyclable nanocomposites for the degradation of organic dye. *Materials*. 7(5):4034-4044.
16. Haider AJ, Jameel ZN, Taha SY. 2015. Synthesis and characterization of TiO<sub>2</sub> nanoparticles via sol-gel method by pulse laser ablation. *J Eng Technol*. 33(5):761-771.
17. Khan A, Adam A, Aziz MA, Ahmed MI, Yamani ZH, Qamar M. 2019. Shape-dependent performance of gold nanocrystals supported on TiO<sub>2</sub> for photoelectrochemical water oxidation

- under different radiations. *Int J Hydrog Energy*. 44(41):23054-23065.
18. Patri A, Umbreit T, Zheng J, Nagashima K, Goering P, Francke-Carroll S, *et al.* 2009. Energy dispersive X-ray analysis of titanium dioxide nanoparticle distribution after intravenous and subcutaneous injection in mice. *J Appl Toxicol*. 29(8):662-672.
  19. Li X, Zhu D, Wang X. 2007. Evaluation on dispersion behavior of the aqueous copper nano-suspensions. *J Colloid Interface Sci*. 310(2):456-463.
  20. Chellappa M, Anjaneyulu U, Manivasagam G, Vijayalakshmi U. 2015. Preparation and evaluation of the cytotoxic nature of TiO<sub>2</sub> nanoparticles by direct contact method. *Int J Nanomedicine*. 10(1):31.
  21. Albukhaty S, Al-Bayati L, Al-Karagoly H, Al-Musawi S. 2020. Preparation and characterization of titanium dioxide nanoparticles and *in vitro* investigation of their cytotoxicity and antibacterial activity against *Staphylococcus aureus* and *Escherichia coli*. *Anim Biotechnol*. Published online. Nov. 28:1-7.
  22. Jin CY, Zhu BS, Wang XF, Lu QH. 2008. Cytotoxicity of titanium dioxide nanoparticles in mouse fibroblast cells. *Chem Res Toxicol*. 21(9):1871-1877.
  23. Bermejo-Nogales A, Connolly M, Rosenkranz P, Fernández-Cruz M-L, Navas JM. 2017. Negligible cytotoxicity induced by different titanium dioxide nanoparticles in fish cell lines. *Ecotoxicol Environ Saf*. 138:309-319.
  24. Huang S, Chueh PJ, Lin YW, Shih TS, Chuang SM. 2009. Disturbed mitotic progression and genome segregation are involved in cell transformation mediated by nano-TiO<sub>2</sub> long-term exposure. *Toxicol Appl Pharmacol*. 241(2):182-194.
  25. Yedjou CG, Tchounwou CK, Haile S, Edwards F, Tchounwou PB. 2010. N-acetyl-cysteine protects against DNA damage associated with lead toxicity in HepG2 cells. *Ethn Dis*. 20(1):S1.
  26. Wu Y, Chen Z, Darwish WS, Terada K, Chiba H, Hui SP. 2019. Choline and ethanolamine plasmalogens prevent lead-induced cytotoxicity and lipid oxidation in HepG2 Cells. *J Agric Food*. 67(27):7716-7725.
  27. Assi MA, Hezmee MNM, Abd Wahid Haron MYM, Sabri MAR. 2016. The detrimental effects of lead on human and animal health. *Vet World*. 9(6):660.
  28. Yedjou CG, Tchounwou HM, Tchounwou PB. 2016. DNA damage, cell cycle arrest, and apoptosis induction caused by lead in human leukemia cells. *Int J Environ Res Public Health*. 13(1):56.
  29. Shakoori AR, Ahmad A. 2013. Cytotoxic and genotoxic effects of arsenic and lead on human adipose derived mesenchymal stem cells (AMSCs). *J Stem Cells Regen Med*. 9(2):29.
  30. Rana MN, Tangpong J, Rahman MM. 2018. Toxicodynamics of lead, cadmium, mercury and arsenic-induced kidney toxicity and treatment strategy: a mini review. *Toxicology reports*. 5:704-713.
  31. Chirinos-Peinado DM, Castro-Bedriñana JI. 2020. Lead and cadmium blood levels and transfer to milk in cattle reared in a mining area. *Heliyon*. 6(3):e03579.
  32. Rodríguez L, Ruiz E, Alonso-Azcárate J, Rincón J. 2009. Heavy metal distribution and chemical speciation in tailings and soils around a Pb–Zn mine in Spain. *J Environ Manage*. 90(2):1106-1116.
  33. Miclean M, Cadar O, Levei EA, Roman R, Ozunu A, Levei L. 2019. Metal (Pb, Cu, Cd, and Zn) transfer along food chain and health risk assessment through raw milk consumption from free-range cows. *Int J Environ Res Public Health*. 16(21):4064.
  34. Qin F, Liu G, Huang G, Dong T, Liao Y, Xu X. 2018. Zinc application alleviates the adverse effects of lead stress more in female *Morus alba* than in males. *Environ Exp Bot*. 146:68-76.
  35. Giergiel M, Lopucki M, Stachowicz N, Kankofer M. 2012. The influence of age and gender on antioxidant enzyme activities in humans and laboratory animals. *Aging Clin Exp Res*. 24(6):561-569.
  36. Du H, Zhu X, Fan C, Xu S, Wang Y, Zhou Y. 2012. Oxidative damage and OGG1 expression induced by a combined effect of titanium dioxide nanoparticles and lead acetate in human hepatocytes. *Environ Toxicol*. 27(10):590-597.
  37. Liu K, Lin X, Zhao J. 2013. Toxic effects of the interaction of titanium dioxide nanoparticles with chemicals or physical factors. *Int J Nanomedicine*. 8:2509.
  38. Zhu Y, Fan W, Zhou T, Li X. 2019. Removal of chelated heavy metals from aqueous solution: A review of current methods and mechanisms. *Sci Total Environ*. 678:253-266.
  39. Salahuddin N, Galal A: Improving chemotherapy drug delivery by nanoprecision tools. *Nanostructures for Cancer Therapy*. Elsevier. 2017:87-128.
  40. Goutam SP, Saxena G, Singh V, Yadav AK, Bharagava RN, Thapa KB. 2018. Green synthesis of TiO<sub>2</sub> nanoparticles using leaf extract of *Jatropha curcas* L. for photocatalytic degradation of tannery wastewater. *Chem Eng J*. 336:386-396.